Numerical Simulation of Instability Characteristic in Pump turbines

Hongjuan Ran, Xianwu Luo, Dezhong Wang

Numerical Simulation of Instability Characteristic in Pump turbines

Hongjuan Ran[1], Xianwu Luo[2], Dezhong Wang[1]

ISROMAC 2016

International Symposium on Transport Phenomena and Dynamics of Rotating Machinery

Hawaii, Honolulu

April 10-15, 2016

Abstract

In classical pumps, there is single positive slope part on the curve of pump performance, named head-drop phenomenon. However, a second head-drop phenomenon is found in our experiments in the pump mode of some medium pump turbines. The flow rate of this second head-drop phenomenon is 0.68 - 0.71 times of the design flow rate. As shown in our experimental results, it is significantly influenced by the complex vortices in the impeller inlet domain. Using SST k-ω turbulence model, numerical simulations are conducted to reveal its mechanism. After comparing numerical simulation results with the experimental results, it can be concluded that this second head-drop is closely related with the complex vortices in the impeller inlet. The complex vortices, due to the transmission flow between separated flow and back flow, is responsible for this second head-drop phenomenon.

Keywords

Head-drop — complex vortices — numerical simulation

[1]*Department of Nuclear Science and technology engineering, Shanghai Jiao tong University, Shanghai, China*

[2]*Department of thermal engineering, Tsinghua University, Beijing, China*

***Corresponding author**: juan@sjtu.edu.cn

INTRODUCTION

Head-drop phenomonon occurs widely in pumps and compressors, and it influences the system's security and reliability. Our paper studies a scaled model of some pump turbine, which is a key component in the hydraulic storage power plant, whose stability influences the flexibility and stability of grid net.

The whole passage of pump turbine includes volute, diffuser, runner and draft tube, which are the same parts with that of general pumps. However, the angles of the diffuser component is adjustable in pump turbines. Hence, there are two head-drops on one performance curve, due to the adjustable angles of the diffuser part, whereas single head-drop is found on one curve of general pumps with the fixed angles of the diffuser part.

Lots of researchers study the head-drop phenomenon with experimental and numerical methodology. Some conclude that rotating stall (near vane less domain between the diffure and the impeller) plays a key role in the head-drop phenomenon in pumps [1, 2, 9, 10, 11, 12,and 13], while other researchers state that the head-drops are closely tied with the flow separation near the runner shroud domain in other pumps [3,4 and 5]. Though lot of experiments study and CFD research are conducted, the mechanism of the head-drop are not clear.

Based on the conclusion of our research, two different head-drops are observed on one curve of pump turbine through experimental study and numerical study [15,16]. This paper investigate the second head-drop phenomonon by methods of numerical simulations. Numerical results are compared with the experimental results. The results show that this second head-drop is caused by the complex vortices in the runner inlet domain. The complex vortices, due to transmission flow between seperated flow and back flow, includes high vortex flow pattern in the impeller inlet. Its detailed mechanism is partly revealed in this paper.

1. METHODS

Numerical simulation with commercial software CFX is conducted on the pump turbine model, based on the study of its experiments' results.

The proper turbulence model is important for predicting the unsteady flow at the off-design conditions for the rotating machine [11] [14] [17]. Numerical simulation comparison among five different rotating models and three different turbulence models are carried out, and their results are compared with experimental results individually, the Shear Stress Transport k-ω turbulence model is demonstrated to simulate this phenomenon more precisely than other models. Shear Stress Transport k-ω turbulence model is adopted in our paper. y^+ range is from 30 to 300, and the main area of fluid flow is 100. Since SST model accounts for the transport of the turbulent shear stress, it is more proper to simulate the flow separation with the consideration of adverse pressure gradients. It captures viscous sublyaer between the solid surface and fluid flow. In our case, based on our analysis of experiments results, the head-drop phenomena is related with separation flow near the impeller inlet domain, especially the cavitation vortices on the shroud surface, and these vortices are supposed to be related with viscous sublayer. Hence, SST k-ω is adopted.

1.1 Study model and boundary set up

The case study is a model of some pump turbine with 9 blades and 20 wicket gates, as shown in Figure 1. Experiments are carried out at test rig of swiss federal institute of technology in Lausanne according to IEC 60193 standard.

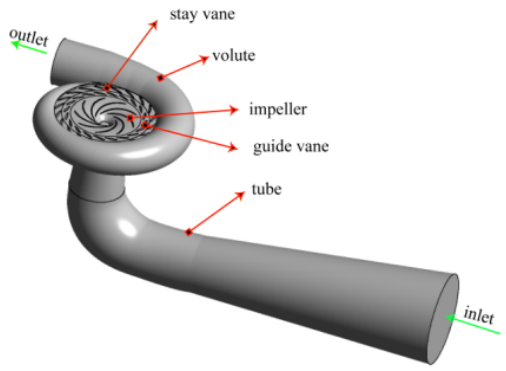

Figure 1. Numerical simulation model with the whole passage of some pump turbine

The uniform flow velocity profile is set at the inlet of calculation domain according to the mass flow. The average pressure at the domain outlet is set. Standard wall function is applied for the near wall, and non-slip condition is set for those solid walls. The simulated flow rate of the valley point is 0.694 Q/Q_{BEP} with wicket gate opening 26°, as described in Figure 2. The time step is set up as one degree of the impeller revolution.

1.2 Grid independence check

Numerical simulation domain includes the whole passages of the pump turbine. Mesh number independent certifies as follows.

Table.1 three different meshes

items	Guide vane	runner	Stay vane	cone	Draft tube	Volute	total
Mesh 1	19943	60243	17037	155700	259638	172773	685334
mesh 2	132714	358420	188623	410172	653700	360396	2104025
mesh 3	738888	1426414	826608	1814089	653700	1443028	6902727

Table.2 Losses in different components

cases	CPrunner	CPvolume	CPdiffuser	CPexcept volute
mesh1	5735	-29	330.15	-333.27
mesh 2	5740	-78.21	327.29	-346.68
mesh 3	5662	-119.8	328.8	-334.29

Pump performance of three different meshes are simulated, and Table 1 shows the different mesh numbers. Table.2 displays the losses in different components. With the consideration of the computer sources and time consumption, mesh 2 is adopted in our simulation.

2. Results comparison

As shown in Figure 2, pump performance are carried out in test rig in Swiss Federal institute of Techonolgy in Lausanne. In Figure 2, there are two curves and each one is with two head-drop parts. These two curves are due to the hysterisis characteristic of head-drop phenoma. The lowest head of the second head-drop part is shown with the black arrow. This paper simulates this valley point to study the characteristic of the head-drop.

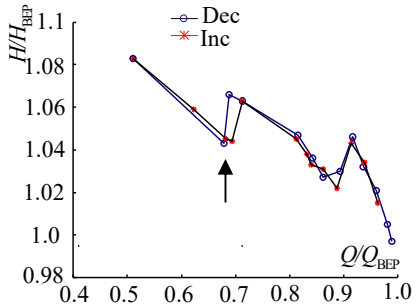

Figure 2. Pump performance curves with two head-drop phenomena with 26° of wicket gates ('Inc' denoted increasing flow rate from part load to full load during experimental procedure; and 'Dec' denoted decreasing flow rate from full load to part load)

Table.3 Pump performance comparison

Test H/H_{BEP}	Simulation $\bar{H}/H_{BEP}$	ε (%)
1.04	1.10	5.50

Table.3 demonstrates the head comparisons between numerical simulation results and experimental results. In the results of the numerical simulation, we choose their average head of different time steps as their compared head. Table.3 shows their error is 5.5%. Their error is caused by the complex flow pattern in the head drop phenomnon, including cavitation, noise and unstable flow.

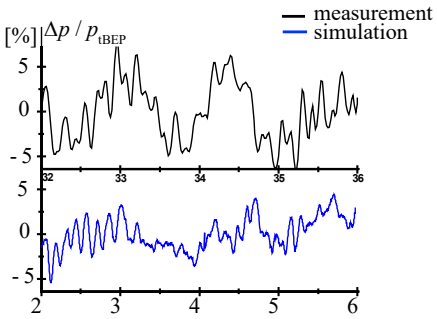

Figure 3. Pressure fluctuation comparison between numerical results and experimental results on the draft tube.

Figure 3 shows pressure flucutation comparison on the draft tube near the runner inet. The x-axis represents the runner revolution, and the y-axis represents the relative amplitude of pressure fluctuation to the pump head of best efficiency point. Two curves are with similar tendancy. Their differences are due to complex flow pattern with cavitation and noise.

3. Results Discussion

3.1 Components head (or loss) versus runner revolution

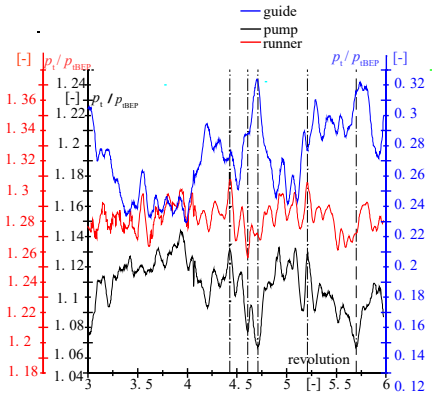

Figure 4. Unsteady numerical simulation results: the distribution of work (or loss) in different passages: guide vanes, runner and whole passage of pump.

Figure 4 shows the work (or loss) of the different components varies with different runner steps. These components include a runner, the wicket gates, and the whole passage of the pump. The vertical coordinate represents the pressure, normalized by the total pressure of the operating point of the best efficiency. With the runner rotating, the pump head vibrates, and the work of the runner and the loss of the wicket gates verifies synchronically. They both cause head-drop phenomonon. It is concluded that the head (or loss) vibrations of the runner and the wicket gates both take responsible for the second head-drop phenomonon. This paper studies the flow pattern of the runner passages, since this flow pattern are also oberved by the experimets.

3.2 Unsteady flow pattern near the runner inlet domain

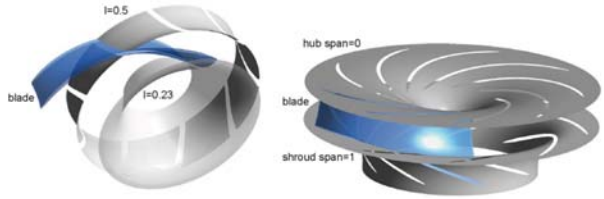

(a) The span value (runner inlet l=0.23; runner outlet l=0.50) and the streamline value (shroud: span =1; hub: span=0)

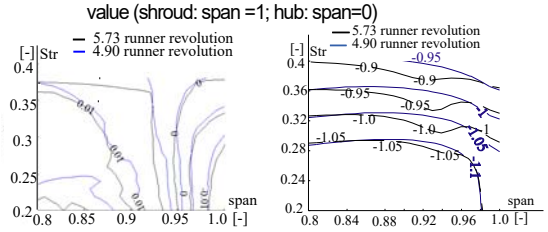

(b). Mass flow contour (c). Pressure contour

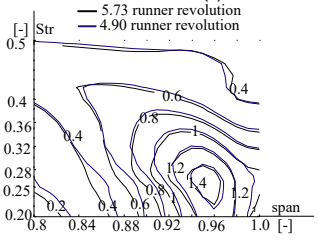

(d). Vortices contour

Figure.5 Contours' comparisons between 4.90r and 5.73r (4.90r stands for the higher value of pump head, and 5.73r denoted the lower value of pump head, as shown in Figure 4) near the shroud domain of the runner

As shown in Figure 5, the different performances between 4.9r and 5.7r (the time steps shown in Figure 4) are displayed. The work of the runner at 4.9r is higher than that in 5.73r (as shown in Figure 4). Figure 5(a) shows the streamline value and the span value corresponded to the position of the runner. The span value of 0 is on the hub, while the span value of 1 is on the shroud. The streamline value from 0.25 to 0.5 corresponded to the runner from the inlet to the outlet. As shown in Figure 5 (b), Figure 5 (c) and Figure 5 (d), The horizontal coordinate shows the span value, and the vertical coordinate represents the streamline value, and these curves in these figures stand for the contour distributions of the mass flow, the pressure and the vortices individually.

As the mass flow distributions of 4.90r and 5.73 r shown in Figure 5 (b), the backflow domain is represented by contour value of -0.01 and no separation domain is denoted by the contour value of 0.01, and contour value of 0 represents the totally blockage flow domain. The seperation domain (contour value less than 0.01 value) is larger in 5.73r than that in 4.90r. So does the totally blocked domain. However, the backflow domain (contour value is larger than 0.01 value) is larger in 4.9r than that in 5.73r. Shortly, the separation flow and blockage flow and complex vortices among them cause the diminish of the runner work in 5.73r. It's must be noted that the backflow seems not harmful for the runner work.

The contour of Figure 5 (c) shows the pressure distribution comparison between 4.90r and 5.73r. From span value 0.90 to span value 0.97, The pressure value is less in 5.73 r than that in 4.90r during this range of span, corresponding to the dramatically unsteady flow pattern in Figure 5 (b).

Figure 5 (d) shows the Vortices distribution comparison between 4.90r and 5.73r. Near the runner leading edge (stream value from 0.25 to 0.28), the vortices domain of the same value is larger in 5.73 than that in 4.90r, corresponding to the unsteady flow pattern in Figure 5(b) and pressure distribution in Figure 5(c). The change of the complex vortices is significantly important for the head-drop phenomonon.

Briefly, the complex flow near runner inlet varies with the impeller rotating, and so do the runner performances, such as pressure and mass flow. Hence, the complex vortices induce the vibration of the impeller work, which further causes the head-drop.

3.2 Complex vortices near the runner inlet domain

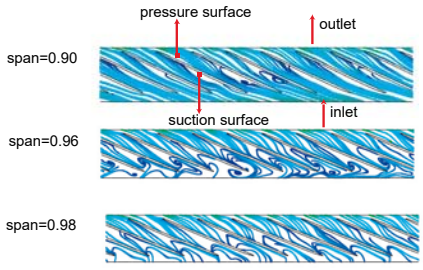

(a) Streamlines in several spans near the shroud domain

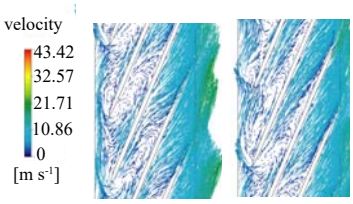

(b) Velocity near the shroud domain (span=0.96)

Fig. 6 several flow patterns in runner passages near the inlet domain, And the time step is 4.9 runner revolution step (as shown in Figure 4).

Figure. 6 shows different flow patterns occured in the runner inlet domain. They include the well flow, the separated flow, the complex vortices and the back flow.

As shown in Figure 6 (a), there are several different flow patterns with the span value 0.90 - 0.97. As shown in Figure 6 (a) with the span value 0.9, some vortex occur in the middle of the passage, near the suction surface of the impeller. The flow pattern are also similar with the span value 0.6 - 0.9; At the span value 0.96, the flow becomes complex, which includes three parts:

A part of the flow in one passage flows to the adjcent passage, and they are totally blocked, coressponding to Figure 6 (b). A part of the flow developes new vortex because they collapes with the leading edge of the baldes.

Another part of these seperated flow generates a circulating flow, which flows around the circle band near the impeller inlet (as shown in Figure 6 (b)). and these complicated flow changes significantly with the different time steps (as shown in Figure 5).

The flow is back flow near the shroud domain, and it is from the runner inlet to the draft tube cone, as shown in third image of Figure. 6 (a).

Briefly, the complex vortices, with high value Vortices and high performance of instability, (as shown in Figure 6 (a)) are caused by the transition flow pattern from the initial separation flow to the backflow. It is concluded that the transition flow induces the second head-drop phenomonon.

4 Conclusions

This paper study the head-drop phenomonon of a pump turbine. The flow rate of the head-drop is from 0.68 Q_{BEP} to 0.71 Q_{BEP}. Its valley point is 0.68 Q_{BEP}, which is as the simulated point. Pump head comparisons between numerical results and experimental results are carried out, and their error is 5%. The pressure fluctuation near the impeller inlet are also compared between numerical results and experimental results, and they are with similar tendency. The errors between numerical and experimental results due to the complex flow pattern with cavitation and noise, yet the numerical simulation doesn't consider the influence of cavitation and noise.

The results of numerical simulation demonstrate that the transition flow in the runner inlet domain causes the head-drop phenomenon. The transition flow are transmission flow from seperated flow to back flow near the runner inlet domain. The transition flow is very complex. It includes the leakage flow from one passage to the adjecent passage, the blocked flow near the blade inlet, the high vortex flow near the blades' leading edges, the circulating flow near the runner inlet domain and little back flow near the shroud domain.

Acknowledgments

The author really appreciates the help from the lab for hydraulic machine in EFPL, the Chinese natural science funding, Industrial funding provided by HEC, China.

References

[1] Cao, S., Goulas, A., Wu, Y., Tsukamoto, H., Peng, G., Liu, W., Zhao, L., and Cao, B., (1999), Three-Dimensional Turbulent Flow in a Centrifugal Pump Impeller Under Design and Off-Design Operating Conditions, *FEDSM-6872 Proceedings of the ASME Fluids Engineering Division*, July 18–23, San Francisco.

[2] Eisele, K., Zhang, Z., Casey, M. V., Gu¨lich, J., Schachenmann, A., (1997), Flow Analysis in a Pump Diffuser-Part1: LDA and PTV Measurements of the Unsteady Flow, *ASME J. Fluids Eng.*, Vol.119 (4):968–977.

[3] Goto, (1992a), Study of Internal Flows in Mixed-Flow in Mixed-Flow Pump Impellers with Various Tip Clearances Using Three-Dimensional Viscous Flow Computations, *ASME Journal of Turbomachinery*, 114:373-382.

[4] Goto, (1992b), The Effect of Tip Leakage Flow on Part-Load Performance of a Mixed-Flow Pump Impeller, *ASME Journal of Turbomachinery*, 114:383-391.

[5] Goto, (1994), Suppression of Mixed-Flow Pump Instability and Surge by the Active Alteration of Impeller Secondary Flows. *Journal of Turbomachinery*,116/621.

[6] Hergt, P. and Benner, R. , (1968), Visuelle Untersuchung der Strömung in Leitrad einer Radialpumpe. Schweiz. Banztg., Vol.86:716--720.

[7] Kevin A. Kaupert, (1999), Turbomachinery Laboratory, ETH Swiss Federal Institute of Technology, Swithzerland, Thomas Staubili, The unseady pressure field in a high specific speed centrifugal pump impeller --- part I: influence of the volute, *Journal of Fluids Engineering*, Vol.121.

[8] Lenneman, E. and Howard, J. H. G., (1970), Unsteady flow phenomena in centrifugal impeller passages. ASME J. Eng. for Power, Vol.92.1:65--72.

[9] Longatte F., and Kueny J. L., (1999), Analysis of Rotor Stator Circuit Interactions in a Centrifugal Pump, FEDSM-6866, *ASME Fluids Eng. Conf.*, San Francisco.

[10] Masamichi Iino, Kazuhiro Tanaka, (2004), Numerical analysis of unstable phenomena and stabilizing modification of an impeller in a centrifugal pump. *22nd IAHR Symposium on Hydraulic Machinery and Systems*, Stockholm – Sweden.

[11] Miyake, Y., and Nagata, T., (1999), Full Simulation of a Flow in a Single Stage Axial-Rotor in Rotating Stall, FEDSM-7197, *ASME Fluids Eng. Conf.*, San Francisco.

[12] Murai, H., (1968), Observations of cavitation and flow patterns in an axial flow pump at low flow rates (in Japanese). Mem. Inst. High Speed Mech., Tohoku Univ., Vol.24 (246):315--333.

[13] O.Braun, (2009), Part-Load Flow in Radial Centrifugal Pumps, thesis no 4422, EPFL, Swiss.

[14] Pinarbasi, K. M. G. A, (2004), Numerical simulations

of the stalled flow within a vaned centrifugal pump, Proceedings of the institution of mechanical engineers part c-*Journal of Mechanical Engineering Science*, Vol.218: 425.435.

[15] Ran HJ, (2010), Study on Double positive slopes phenomena in pump turbines, thesis, Tsinghua University, China.

[16] RAN Hongjuan, LUO Xianwu, ZHU Lei, ZHANG Yao, WANG Xin, and XU Hongyuan. Experimental Study of the Pressure Fluctuations in a Pump Turbine at Large Partial Flow Conditions. *Chinese Journal of Mechanical Engineering 2012 25(6)*: 1205-1

[17] Xiao Yexiang, Wang Zhengwei, Yan Zongguo. Experimental and Numerical Analysis of Blade Channel Vortices in a Francis Turbine Runner. *Engineering Computations*, 2011, 28(2):154-171.